①

AD-A221 918

Kinetic Nonlinearities in Nonuniform Plasmas

G.J. Morales and J.E. Maggs

PPG-1297   April 1990

University of California at Los Angeles
Department of Physics
Los Angeles, CA 90024-1547

90 05 02 027

KINETIC NONLINEARITIES IN NONUNIFORM PLASMAS*

G. J. Morales and J. E. Maggs

Physics Department, University of California, Los Angeles
Los Angeles, CA   90024

INTRODUCTION

The properties of basic kinetic nonlinearities (e.g., particle trapping, nonlinear Landau damping, etc.) in uniform plasmas are well understood, and an extensive literature exists on the subject.[1-3] However, in many problems of current interest, plasma nonuniformity plays an important and fundamental role. Although helpful insight can often be obtained using local, or WKB generalizations of nonlinear phenomena in uniform media, such extrapolations often miss important features. Consequently it is of interest to develop a systematic study of nonlinear phenomena in the context of a well-defined problem in which the intrinsic plasma nonuniformities are retained without undue complexity. Clearly there are numerous topics to be considered in this area, and in recent years we have analytically and numerically investigated a few key issues motivated by broader research interests.   This manuscript presents an abbreviated summary of the highlights of these studies.

Our studies of kinetic nonlinearities in nonuniform plasmas have been motivated, in large measure, by several experimental observations which have not yet been fully explained quantitatively from first-principles calculations.   Prominent among these are issues related to wave generation, possibly by distortions in the electron distribution function.   In laser-plasma experiments, an ongoing assessment is being made[4,5] of anomalies observed in the spectral features of Raman scattering which can not be explained by conventional parametric instability theories. In ionospheric modification experiments that use powerful ground-based HF transmitters, anomalies are also observed[6,7] in the wave spectrum sampled by radar backscattering. Typically, frequencies different than that of the HF wave are observed, and are not trivially related to parametric instabilities.   In such

---

experiments, stimulated electromagnetic emissions[8] are also observed over a broad frequency band.

Another topic that has motivated our investigations is electron acceleration by waves in nonuniform plasmas. In the topside ionosphere, spontaneous generation of fast field-aligned electron bursts have been observed.[9] We speculate that the underlying mechanism involves whistler wave mode conversion in low density plasma irregularities. Also, various aspects of beat-wave excitation are currently being considered in regards to features introduced by plasma nonuniformity.

PHYSICAL MODEL

In surveying the literature of wave-particle interactions in nonuniform media, many studies are found to be deficient because the source of wave generation is ill-defined, and the boundary conditions are not well-posed. Regrettably, some otherwise fine studies confuse the meaning of temporal and spatial nonlinearities and are thus unable to make concrete predictions in spite of significant analysis. To overcome these shortcomings, without introducing unnecessary complexity, we use a simple model in our studies in which wave generation and the essential role of plasma nonuniformity are retained. We consider the model to be a "theoretical laboratory" in which one can systematically study various kinetic nonlinearities in a universal scaled form, so that meaningful comparisons to a variety of experimental scenarios can be established.

The essence of the model is illustrated in Figure 1. It consists of a plasma with a linear density profile $n_0(z)$, having scale length L in the neighborhood of the spatial point $z = 0$, where the local plasma frequency ω_p matches the frequency ω of an external source, $S(z) \exp(-i\omega t)$. We envision the density gradient to be supported by low energy electrons because, conceptually, they have a relatively short collision mean free path. To extract interesting effects related to wave-particle interactions we assume the presence of energetic electrons (fast tail electrons) whose density n_t is spatially uniform and small compared to the low-velocity electron density, $n_t << n_0$. The assumption of uniform density for fast electrons rests upon their collision lengths being much longer than the scale lengths of the wave structures generated in the plasma. The spirit of the model is to treat the

response of the slow electrons through a warm-fluid description, involving a differential equation in configuration space, while the tail electrons are treated kinetically in Fourier transform space.

External Pump
Sets frequency ω

$S(z) \exp(-i\omega t)$
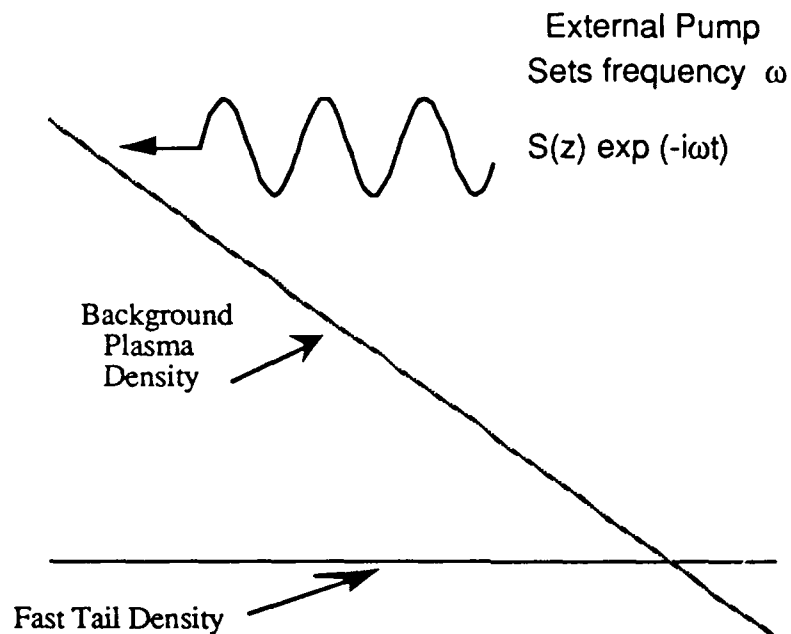
Background
Plasma
Density

Fast Tail Density

Figure 1. The plasma model consists of a cold plasma with a density gradient and a hot uniform tail.

The spatial dependence of the source function $S(z)$ used to resonantly excite plasma waves can model several physically interesting situations of experimental relevance. By choosing $S(z)$ constant, the model rigorously describes the process of linear mode conversion of an oblique electromagnetic wave[10] into a Langmuir wave (as in laser-plasma studies) in an unmagnetized plasma, or the mode conversion of an oblique electrostatic whistler wave[11] into a Langmuir wave in a magnetized plasma. The choice of a sinusoidal $S(z)$ can describe beat excitation by transparent electromagnetic waves (up or down the density profile) as well as direct conversion[12] on density ripples.

SLOPE REVERSAL

The self-consistent resonant electric fields excited in the

presence of a small population of tail electrons is obtained from the solution of a differential equation in Fourier transform space (k-space).

$$\left[\frac{i}{L}\frac{d}{dk} + i\Gamma - \frac{3k^2}{k_D^2} + i4\pi Im\ \tilde{\chi}_t \right] \tilde{E}(k,\omega) = E_0\ \tilde{S}(k)\ ,\qquad (1)$$

where Γ represents collisional damping, and k_D is the Debye wavenumber, $\tilde{\chi}_t$ is the susceptibility of the tail electrons and its effect in (1) is to describe Landau damping. Equation (1) can be solved analytically and then inverted numerically to obtain the spatial pattern $E(\xi)$, where the relevant scaled spatial coordinate is $\xi = (k_D L/\sqrt{3})^{2/3}\ z/L$. Figure 2.a exhibits the spatial dependence of the field amplitude for the case corresponding to linear mode conversion (constant S). The top curve corresponds to the undamped situation (no collisions, no tail), the middle curve contains collisional damping (but no tail), and the bottom curve contains collisional and Landau damping. It is evident collisions cause a reduction in the peak response near resonance where the effective phase velocity is large. Wave-particle interactions with the tail electrons are responsible for damping the mode-converted Langmuir wave as its local phase velocity decreases with distance away from the resonance point. The parameter α is the scaled tail density, $\alpha \equiv (n_t/n_0)\ (\pi/2)^{1/2}\ (k_D L)(\ \overline{v}/v_t)$, with $\overline{v}$, v_t the thermal velocity of the slow and tail electrons respectively.

Figure 2.b exhibits the electric field pattern of a Langmuir wave generated through beat excitation with a wavenumber vector k_b that points in the direction of decreasing density. In this case, local enhancement of the field occurs in the neighborhood of the WKB matching point, and tail Landau damping eventually destroys the unidirectional plasma wave. This wave-particle interaction results in a distortion of the tail distribution and gives rise to a heat-flux to be described later.

When the beat wave number vector points in the direction of increasing density, the excited Langmuir wave initially propagates to its cutoff point (i.e., $\omega_p(z) = \omega$) where it reflects, and then proceeds to propagate in the direction of decreasing density. The corresponding partially-standing wave pattern is shown in Fig. 2.c. In this case wave-particle interactions occur with fast
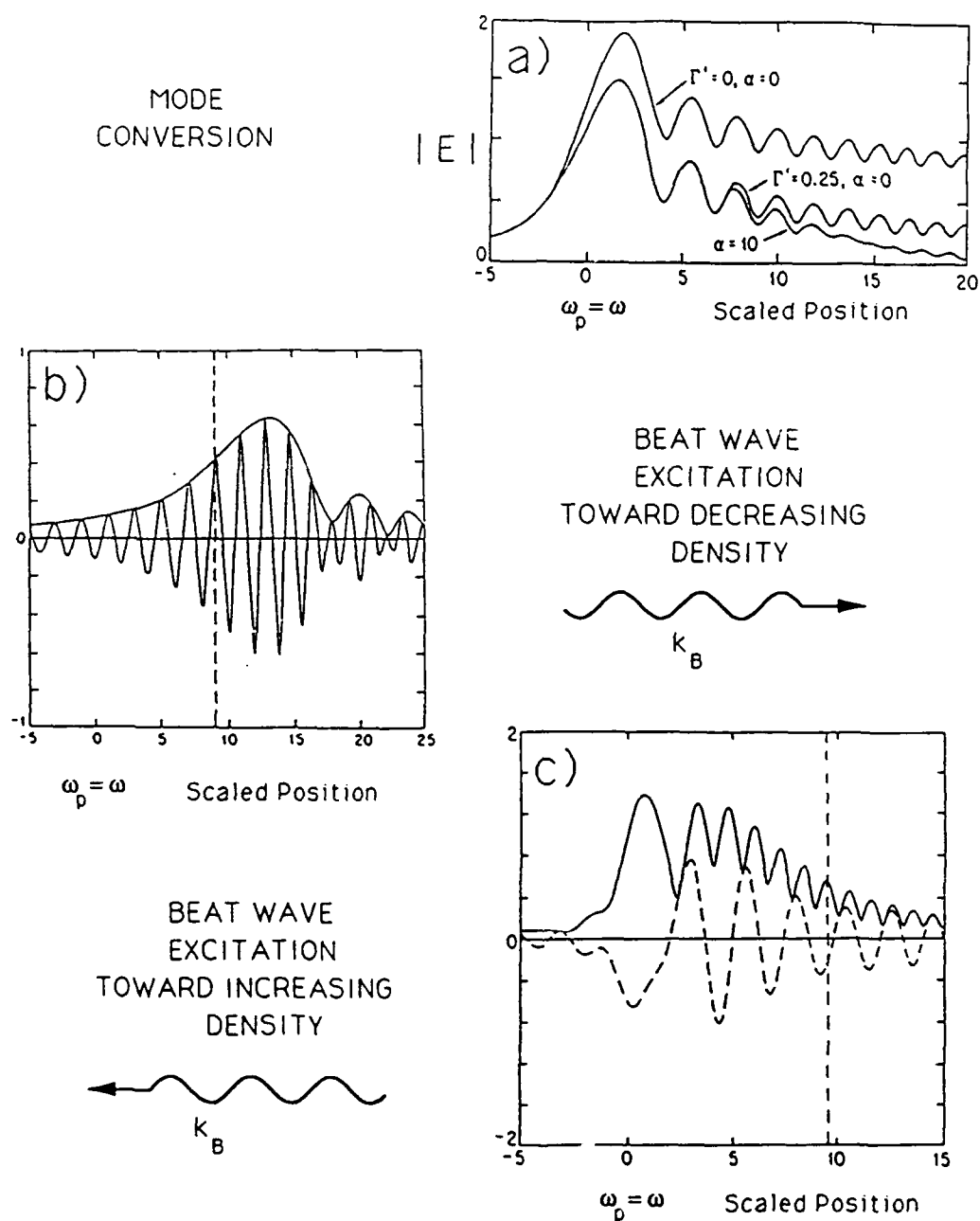
MODE
CONVERSION

BEAT WAVE
EXCITATION
TOWARD DECREASING
DENSITY

k_B

BEAT WAVE
EXCITATION
TOWARD INCREASING
DENSITY

k_B

Figure 2. a) The effects of collisional damping ($\Gamma=0.25$, $\alpha=0$) and collisionless damping ($\alpha=10.$) on the mode converted field amplitude. b) the field excited by a beat wave propagating towards decreasing density, and c) towards increasing density.

electrons moving in both directions so that a bi-directional heat flux develops.

Once the self-consistent, resonantly excited fields have been determined it is possible to calculate the second order (in pump-field amplitude E_0) modifications[13] in the tail distribution function from

$$< \delta f_t(z \to \pm \infty ,v) > = (\frac{e}{2\,m})^2 \frac{1}{v} \frac{\partial}{\partial v} \left\{ | \tilde{E}(k = \frac{\omega}{v})|^2 \frac{1}{v} \frac{\partial}{\partial v} f_{0t} \right\} . \qquad (2)$$

An interesting feature is the ability to generate a slope reversal in the tail distribution once a threshold field amplitude is exceeded. Slope reversal can occur because the increase in the spectral power density at $k = \omega/v$ can be much faster than the rate of decrease in the zero order tail distribution. Consequently, in a given velocity bin, the number of electrons that are promoted to higher velocities can be larger than the number entering the bin from lower velocities, thus a region of positive slope (bump-in-tail) can develop in the velocity distribution. The exact value of the threshold field is determined from a transcendental equation[13], but roughly its magnitude is $E_0 > p(mv_t^2/\pi eL)$, with $p \sim$ 2-5. A detailed analysis[14] related to ionospheric HF-modification experiments shows that the presently available HF facilities operate at power levels large enough to exceed this threshold, so that bump-in-tail distributions can be expected to develop and contribute to the noise spectrum observed in such experiments. The corresponding observation of this phenomenon in laser-plasma experiments is presently being debated[4,5] by experts.

Figure 3.a shows an example of bump formation associated with mode-conversion (the field pattern is like that shown in Fig. 2.a), while Fig. 3.b shows the corresponding slope reversal obtained from beat-excitation in the direction of decreasing density. As can be seen, modifications occur in the velocity interval $v < \omega/k_b$ because the local phase velocity always remains below this value. Figure 3.c shows a composite distribution function ($v < 0$ corresponds to $z \to -\infty$, $v > 0$ to $z \to +\infty$) in which bump formation results from beat excitation in the direction of increasing density.

MODE
CONVERSION

f_{tail}

a)

$\epsilon_0 = 0$

$\alpha = 10$

0

0   1   2   3

Scaled Velocity

b)

$\epsilon_* \cdot 0$

$\ln f_{tail}$

$\frac{\omega}{k_B}$

0   1   2   3   4   5

Scaled Velocity

BEAT WAVE
EXCITATION
TOWARD DECREASING
DENSITY

c)

$\epsilon_* \cdot 0$

$\ln f_{tail}$

$\frac{\omega}{k_B}$

-5   0   5

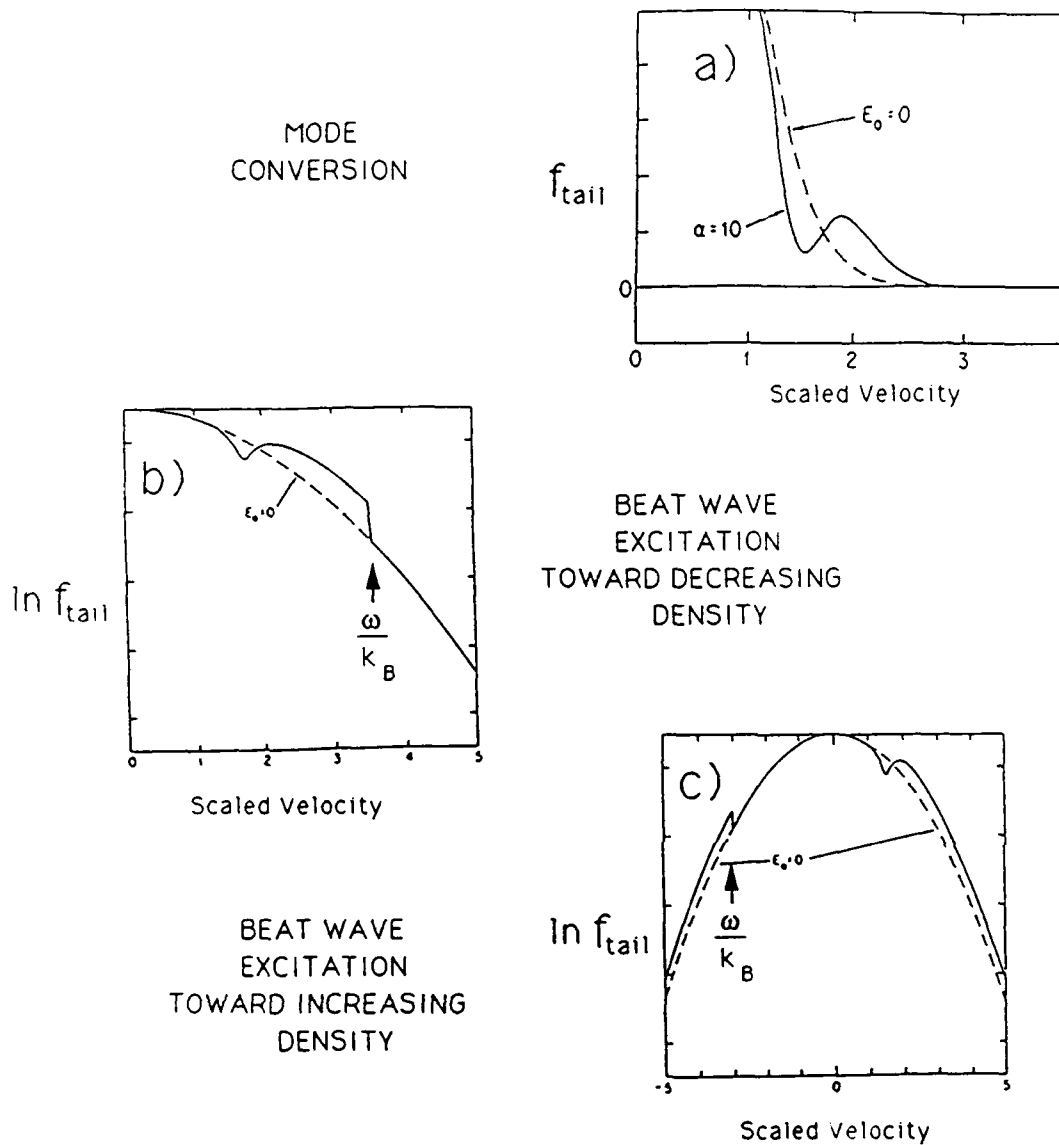Scaled Velocity

BEAT WAVE
EXCITATION
TOWARD INCREASING
DENSITY

Figure 3. a) The electron distribution for $\alpha=10$, b) for a beat wave propagating towards decreasing density, and c) towards increasing density.

EFFICIENCY OF BEAT EXCITATION

Since the physical model describes accurately the self-consistent excitation of Langmuir waves in a density gradient, we have considered the case in which the source $S(z)$ corresponds to the beat-ponderomotive force generated by two transparent ($\omega_j \gg$

ω_p, $j = 1,2$) electromagnetic waves having frequencies ω_j. The resulting beat wave vector k_b can point in either the direction of decreasing (+, for positive z-direction) or increasing (-) density. The modified electron distribution function can be calculated from Eq. (2) to yield[15] the heat flux δQ induced in the plasma by the beat wave process in the ($\pm$) directions

$$\delta Q_{\pm} = \pm \frac{e^2}{4m} \int_0^{\pm\infty} dv \, | \, \tilde{E}(k = \frac{\omega}{v})|^2 \, \frac{\partial}{\partial v} \, f_{0t}^{\pm}(v) \quad . \tag{3}$$

Using the solution of Eq. (1) in Eq. (3) the plasma heating efficiency η for beat wave excitation in a nonuniform plasma can be determined analytically. The compact simple expression for ($\pm$) excitation is

$$\eta_{\pm} = \eta_0 \left\{ 1 - \exp[-2\alpha(1 \mp \exp(-w^2))] \right\} \quad , \tag{4}$$

where $w = (\omega_1 - \omega_2)/\sqrt{2}k_D v_t$, α is given in the discussion of Fig. 2, and

$$\eta_0 = 2\pi \left(\frac{\omega_1 - \omega_2}{\omega_j} \right)^5 (k_{0j}L) \frac{P_2}{n_0 mc^2} \quad , \tag{5}$$

with k_{0j} the wavenumber of the jth wave, P_2 the power density carried by ω_2, and c the speed of light. In the limit of large α, i.e., long scale length L, the efficiency predicted by Eq. (4) reduces to the expression previously found by Rosenbluth and Liu[16], which scales linearly with L. However, in the limit of small α, i.e., short scale length, Eq. (4) predicts a transition to a scaling proportional to L^2.

BUMP-ON-TAIL RESONANT EXCITATION

Motivated by the finding that slope reversal can be produced in the fast-tail electron distribution by resonant excitation, we have investigated the subsequent modifications to the mode conversion process (constant S, Fig. 2.a) when a bump-

on-tail is present. The issues of interest are: 1) Determination of the net amplification resulting from the convective instability driven by the slope reversal; 2) Modifications in the fast-tail distribution due to changes in the pump field amplitude, E_0. For
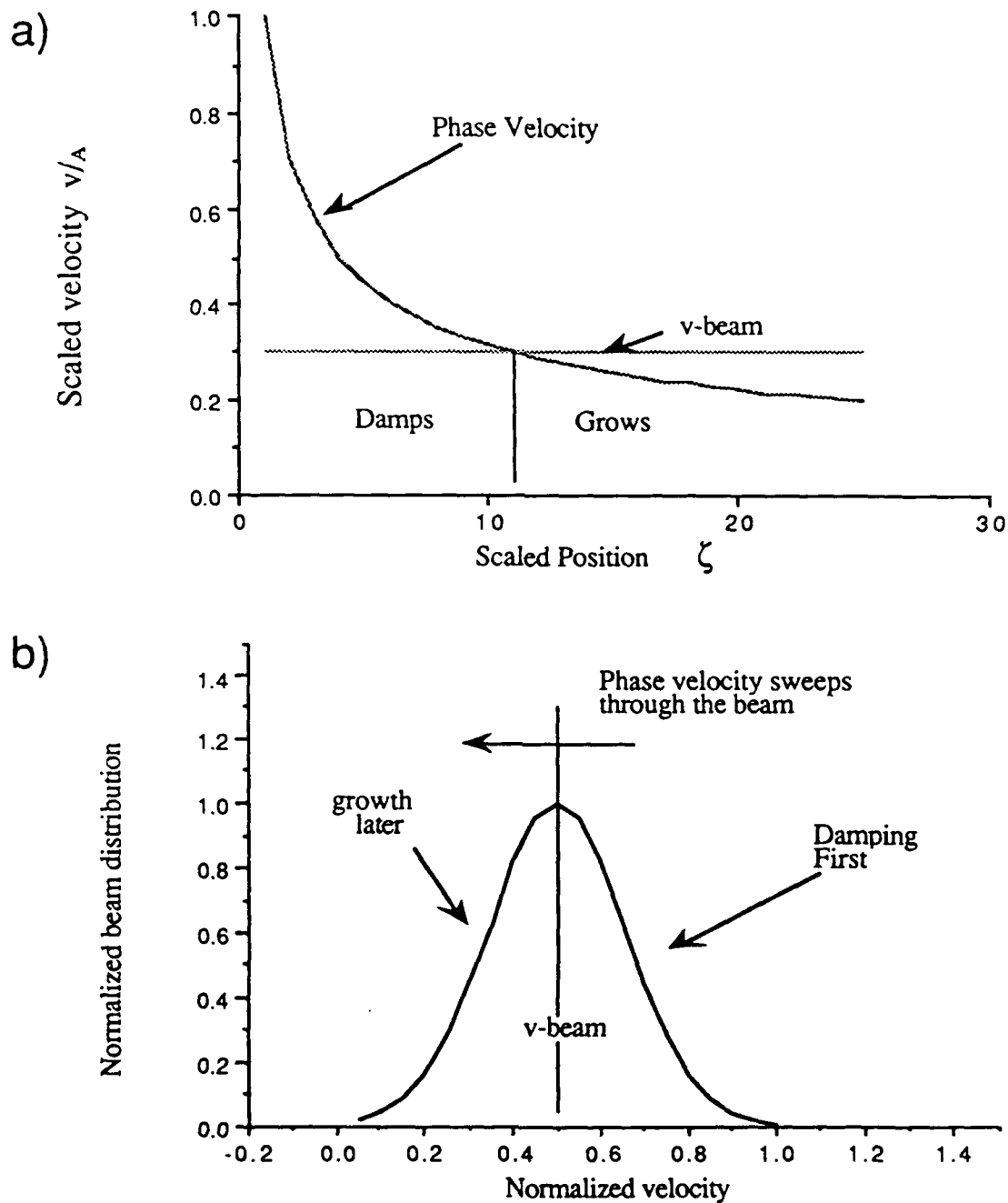
a)

b)

Figure 4. The spatial varying phase velocity results in first damping and then growth from a beam distribution.

concreteness we present the results produced by a beam distribution of the form,

$$f_b(v) = \frac{n_b}{(2\pi \overline{v}_b^2)^{1/2}} \ \exp \ \{-(v-v_b)^2/2\overline{v}_b^2) \} \ , \tag{6}$$

with $n_b \ll n_0$. Mathematically, the beam effects are introduced through the susceptibility $\widetilde{\chi}_t$ in Eq. (1).

The underlying physics of this problem is illustrated in Fig. 4. Figure 4.a shows the spatial dependence of the phase velocity of the wave excited by mode conversion, i.e., $\omega/k(z) \sim z^{-1/2}$, and the unperturbed velocity v_b of the peak of the beam, i.e., where $\partial f_b/\partial v = 0$. In the spatial region near plasma resonance (i.e., $z = 0$), $\omega/k > v_b$ and the wave is damped by the beam because it samples the negative slope region of the distribution. However, at some positive value of z, $\omega/k < v_b$, and in this region wave amplification occurs because the wave samples the positive slope region of the beam distribution. A complementary view is illustrated in Fig. 4.b, which emphasizes that the phase velocity of
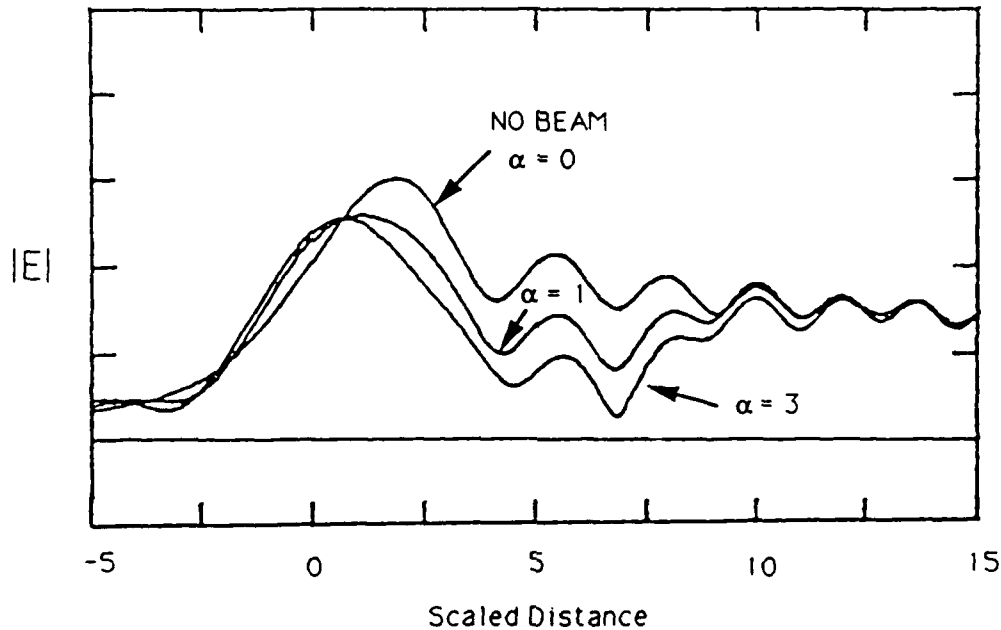

Figure 5. Effect of beam on the mode converted field amplitude for densities corresponding to $\alpha = 1.$, and $\alpha = 3$.

the wave continuously sweeps through the beam velocity distribution, first starting in the damping region so that the fast part of the beam is accelerated, and then proceeding to the growth region in which the slower beam electrons are decelerated.

The effect of the beam on the amplitude of the resonantly excited field is illustrated in Fig. 5 for two values of the scaled beam density α (as defined in the discussion of Fig. 2) with $v_b / \bar{v}_b$ = 5, and $v_b = 2v_A$, where $v_A = \omega L/(k_D L/\sqrt{3})^{2/3}$ is the maximum phase velocity of the field (determined by the width of the Airy pattern at $z = 0$). It is evident that as the beam density increases, the peak amplitude of the resonance decreases and the mode converted wave initially experiences strong damping, as anticipated from Fig. 4. The regrowth of the wave indeed occurs (around $\xi \approx 7$), but with the remarkable signature that asymptotically the amplitude returns to the value obtained in the absence of the beam. This implies that, although there is spatial rearrangement of the wave energy, there is no net gain produced by the beam. This property can be demonstrated analytically to be rigorously correct and independent of the beam distribution parameters for symmetric (about the beam drift velocity v_b) beam distributions. Selective alteration of beam symmetry can
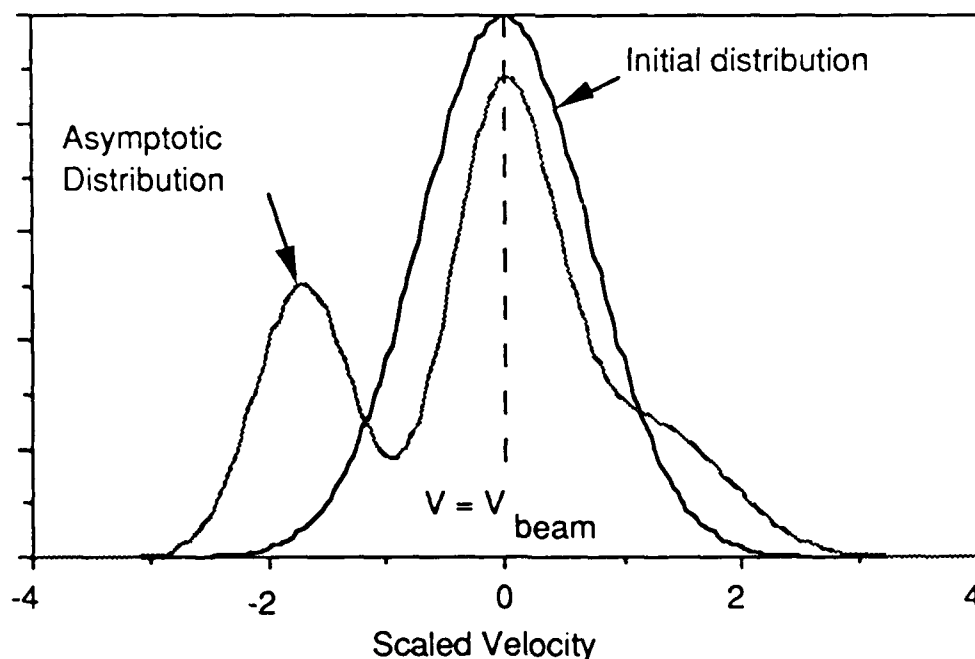

Figure 5. The beam velocity distribution changes as a result of its interaction with the resonant field.

lead to either enhanced damping or growth of the resonant field (these results are not shown here).

Although a symmetric beam does not yield net wave amplification, the resonantly excited wave does modify the beam distribution function as illustrated in Fig. 6 for a scaled pump amplitude $(\pi L e E_0 / \sqrt{2} m\ \bar{v}_b^2) = 5$. It is seen that a few of the beam electrons are accelerated to higher velocities, while a significant number are decelerated during the process of wave regrowth. Beyond some threshold value of E_0 (equivalent to that found for slope reversal) which is exceeded in this example, a multiple-beam distribution is formed.

NONLINEAR LANDAU DAMPING OF RESONANT FIELDS

Since the effective phase velocity of a resonantly excited electric field near plasma resonance scales as $\bar{v}_e/(k_D L)^{1/3}$, the mode converted wave is essentially undamped in plasmas having
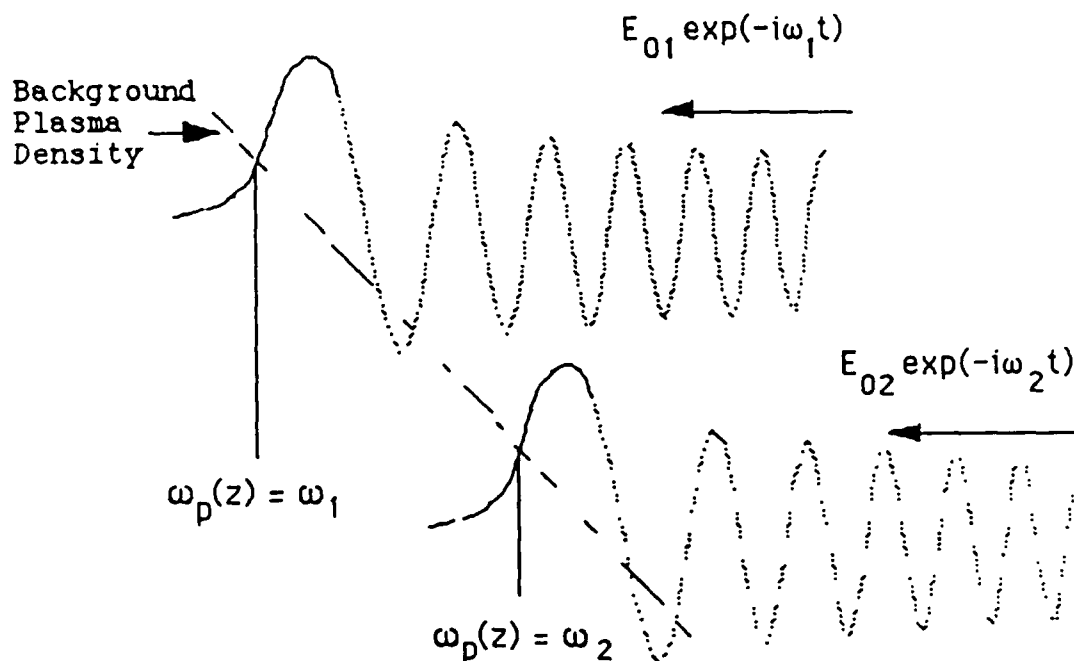

Figure 7. Two external sources having amplitudes E_{01} and E_{02} and frequencies ω_1 and ω_2 drive in resonant field patterns at two separate spatial locations.

large scale lengths L, as illustrated by the top curve in Fig. 2.a. It is therefore of interest to consider the role of nonlinear (beat) Landau damping in such an environment. Figure 7 illustrates the geometry of a case in which two external sources (uniform pumps) are present with closely spaced frequencies, $\omega_1 > \omega_2$, and excite individual resonant electric fields of the type shown in Fig. 2.a. The two resonant field structures are linearly weakly damped (by collisions), and propagate with phase velocities $\omega_1/k_1(z)$, $\omega_2/k_2(z)$ which decrease as $z^{-1/2}$, as sketched in Fig. 8.
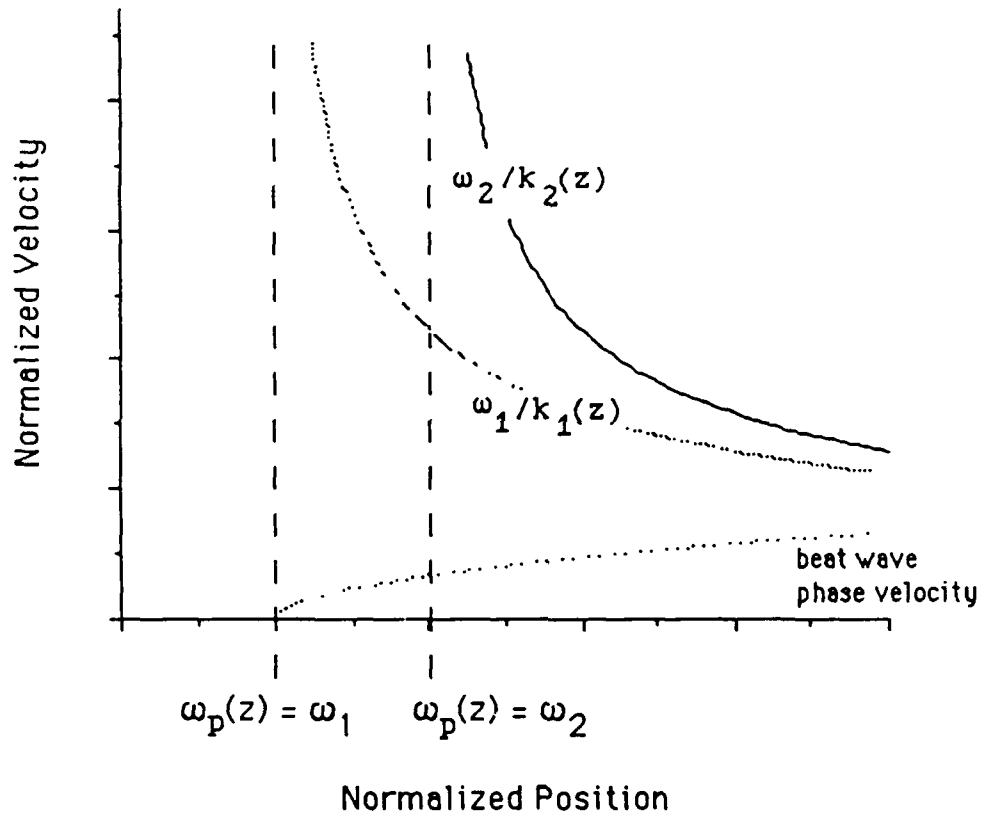

Figure 8. The phase velocity of the beat wave varies as $z^{1/2}$ while the phase velocities of the individual drivers vary as $z^{-1/2}$.

Nonlinearly the waves generate a beat idler whose local phase velocity is $(\omega_1 - \omega_2)/(k_1(z) - k_2(z))$. For small frequency separation the idler phase velocity equals the local group velocity and increases as $z^{1/2}$ and scales as $\bar{v}_e/(k_D L)^{1/3}$. Thus, the idler interacts strongly with slow electrons and background ions.

This problem is presently being investigated by S. Srivastava in his Ph.D. dissertation, and the mathematical details are too lengthy to be presented here. It suffices to say that the formulation consists of three coupled equations to be solved self-consistently for the fields E_1, E_2 oscillating at frequencies ω_1, ω_2, respectively, and the idler field E_3 at frequency $\omega_1 - \omega_2$. The equations for the plasma waves (j = 1,2) are differential equations of the form

$$\frac{3}{k_D^2} \frac{d^2}{dz^2} E_j + \left(\frac{z-z_j}{L} \right) E_j = E_{0j} + S_j(z) \ , \qquad (7)$$

with z_j the cutoff point, E_{0j} the external pump amplitude, and S_j the nonlinear (beat) source arising from coupling to the other two modes. The idler response must be calculated in k-space because of its low effective phase velocity which requires that the response of the ions and slow electrons be described kinetically, giving

$$\frac{i}{L} \left[1 - \varepsilon(\omega_1 - \omega_2, k) \right] \frac{d}{dk} \tilde{E}_3(k) + \varepsilon(\omega_1 - \omega_2, k) \tilde{E}_3(k) = \tilde{S}_3(k) \ , \qquad (8)$$

where ε is the kinetic dielectric and $\tilde{S}_3(k)$ the source in k-space (obtained from a convolution over $\tilde{E}_1 \tilde{E}_2^*$). The relevant nonlinear parameter in the system is $(eE_0L/\sqrt{2}T_e)^2$, where T_e is the electron temperature and, for simplicity, $E_{01} = E_{02} = E_0$. The spatial pattern of nonlinear Landau damping is illustrated in Fig. 9. The top panel shows the amplitude of the individual fields (non-interacting) for $(\omega_1 - \omega_2)/\omega_1 = 0.2$. The middle panel shows the linear and nonlinear (for $(eE_0L/\sqrt{2}T_e)^2 = .15$) amplitudes for the highest frequency wave (i.e., ω_1). It is evident that the nonlinear interaction causes strong damping. The corresponding behavior for the wave at frequency ω_2 is shown in the bottom panel where clear enhancements in the wave amplitude are observed. As expected, the highest frequency wave transfers part of its energy to the lower frequency wave and simultaneously accelerates slow electrons and ions through the idler field. Figure 10 displays the idler field and the power dissipation to both particle species for $T_e/T_i = 1.0$.
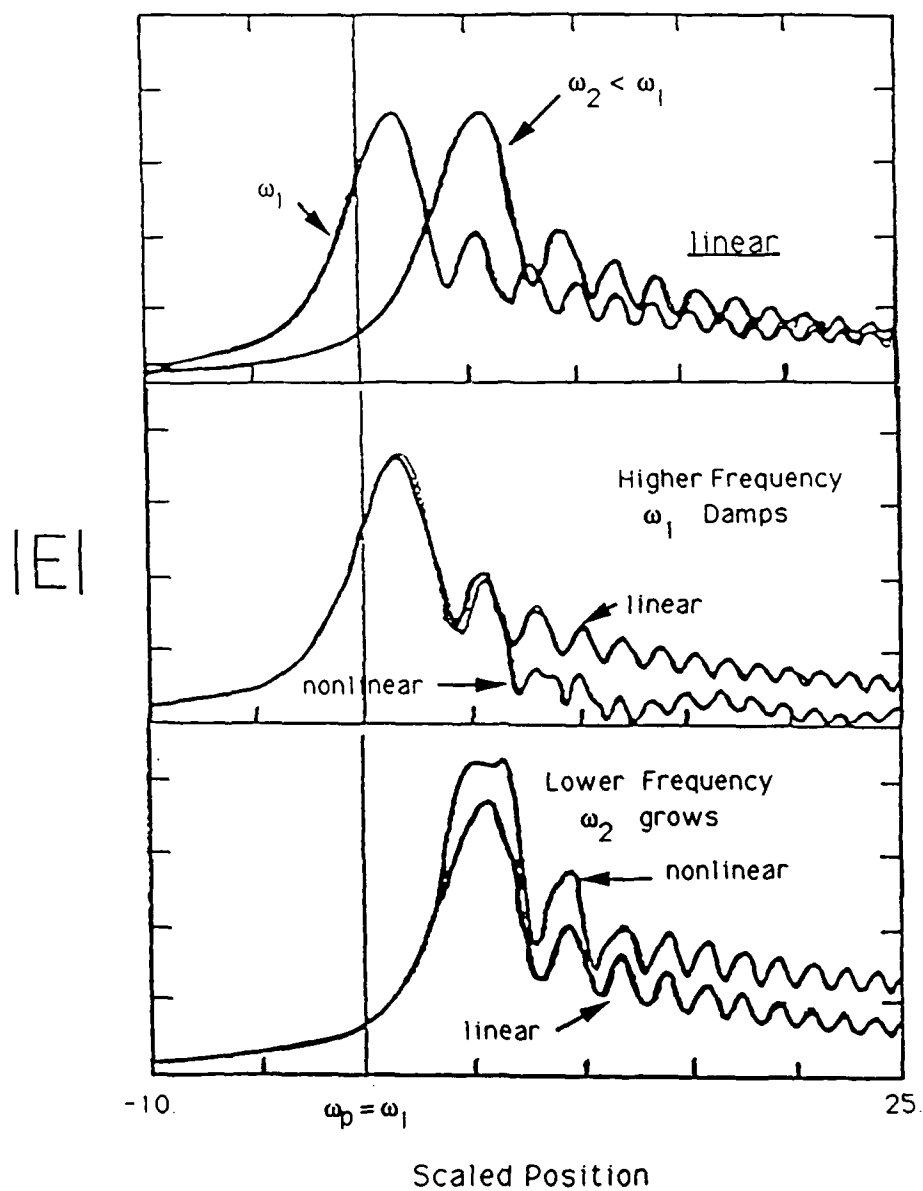
Figure 9. The field amplitude of the two high frequency waves in the linear (top panel) and nonlinear cases (bottom panels).
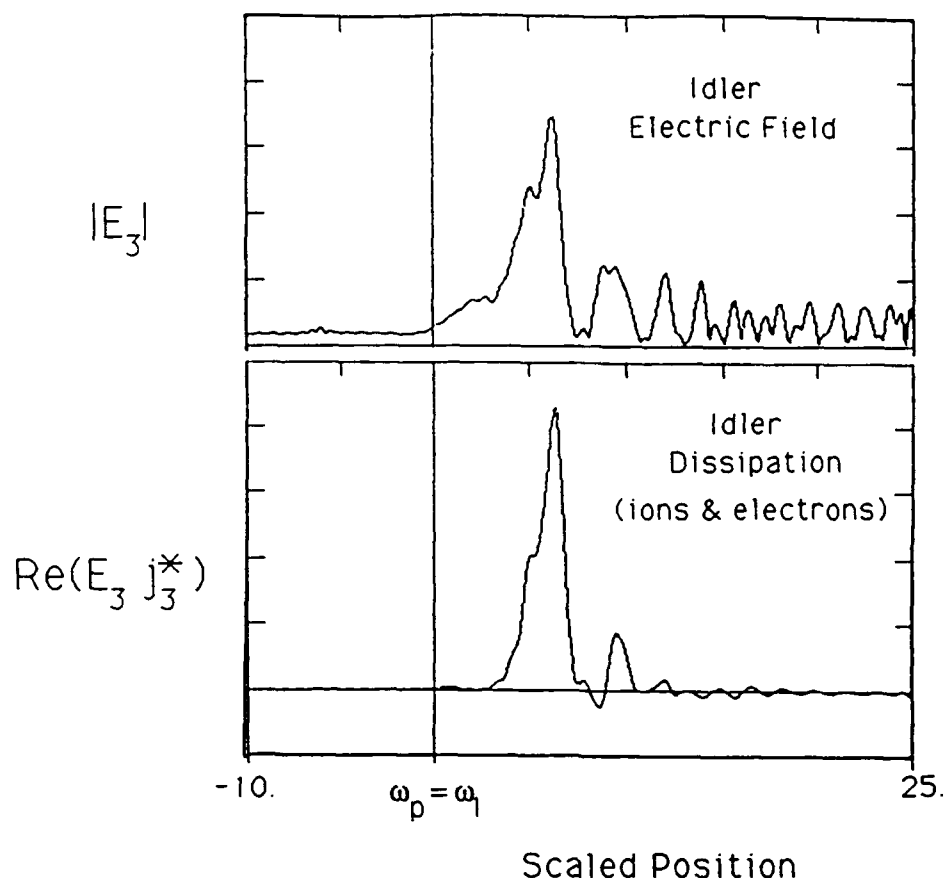
Figure 10. The idler field and spatial pattern of dissipation are shown for a frequency separation of 2% in the driving fields.

NONLINEAR DYNAMICS OF ELECTRONS ACCELERATED BY RESONANT FIELDS

In the analysis of the formation of slope reversal in the electron velocity distribution discussed in Sec. 3, strong wave-particle nonlinearities, such as particle trapping, were not included. To obtain a better understanding of the role strong nonlinearities play in this process, we have performed an extensive numerical and analytical study[17] of individual electron orbits associated with an undamped, driven-Airy pattern whose amplitude corresponds to the top curve in Fig. 2.a. We have found that the nonlinear interactions can be grouped in three categories

depending upon the initial velocity of the particle as illustrated in Fig. 11.

Although the boundaries between the different categories of interaction can be precisely determined the expressions for these boundaries are complicated, so it is convenient to think of the categories as corresponding to fast ($v \geq v_A$), intermediate ($v \approx .5$ v_A), and slow ($v \leq .2v_A$), where the comparison velocity v_A is the
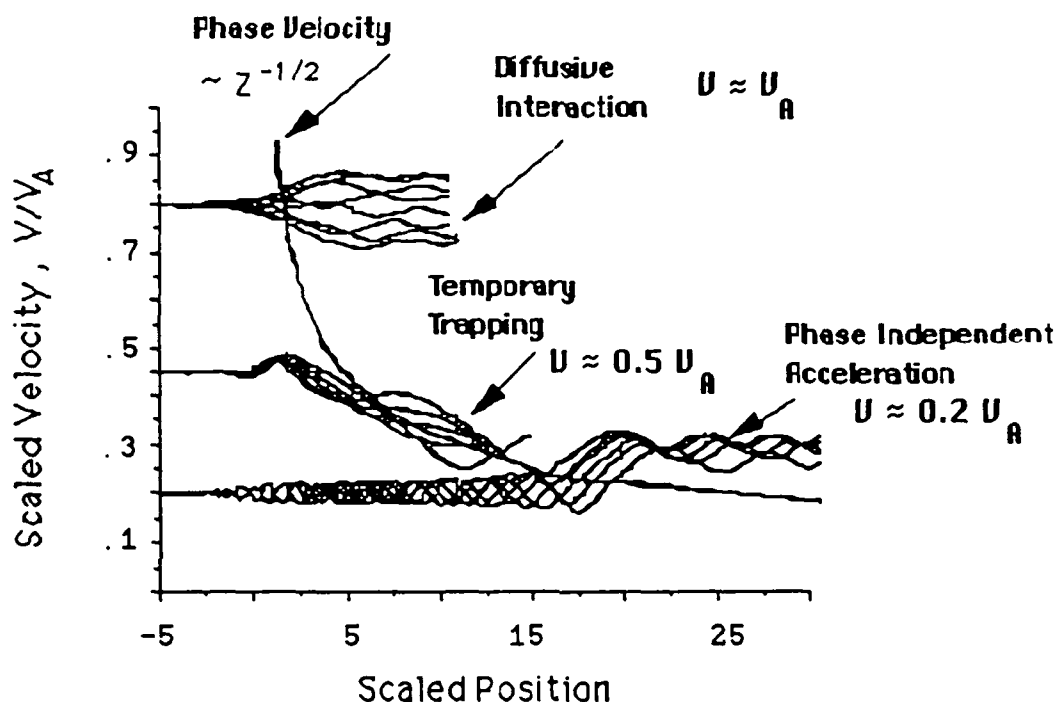

Figure 11. The interactions of particles with a resonant field can be divided into three categories depending upon velocity: fast $V \approx V_A$, intermediate $V \approx 0.5V_A$, and slow $V \approx 0.2V_A$.

fastest phase velocity of the driven-Airy pattern, $v_A \equiv \omega L/(k_D L/\sqrt{3})^{2/3}$. The fast particle trajectory in phase space, as shown in Fig. 11, intersects the phase velocity curve, $v_p \sim z^{-1/2}$, at a very large angle, hence the time of interaction is relatively short, and results in a diffusive interaction in which particles are both accelerated and decelerated as in the second-order theory discussed in Sec. 3. For intermediate velocities it is possible for some particles to be temporarily entrained by the wave. The conditions for this trapping behavior are rather restrictive, occurring only for a narrow velocity and wave-phase range. The
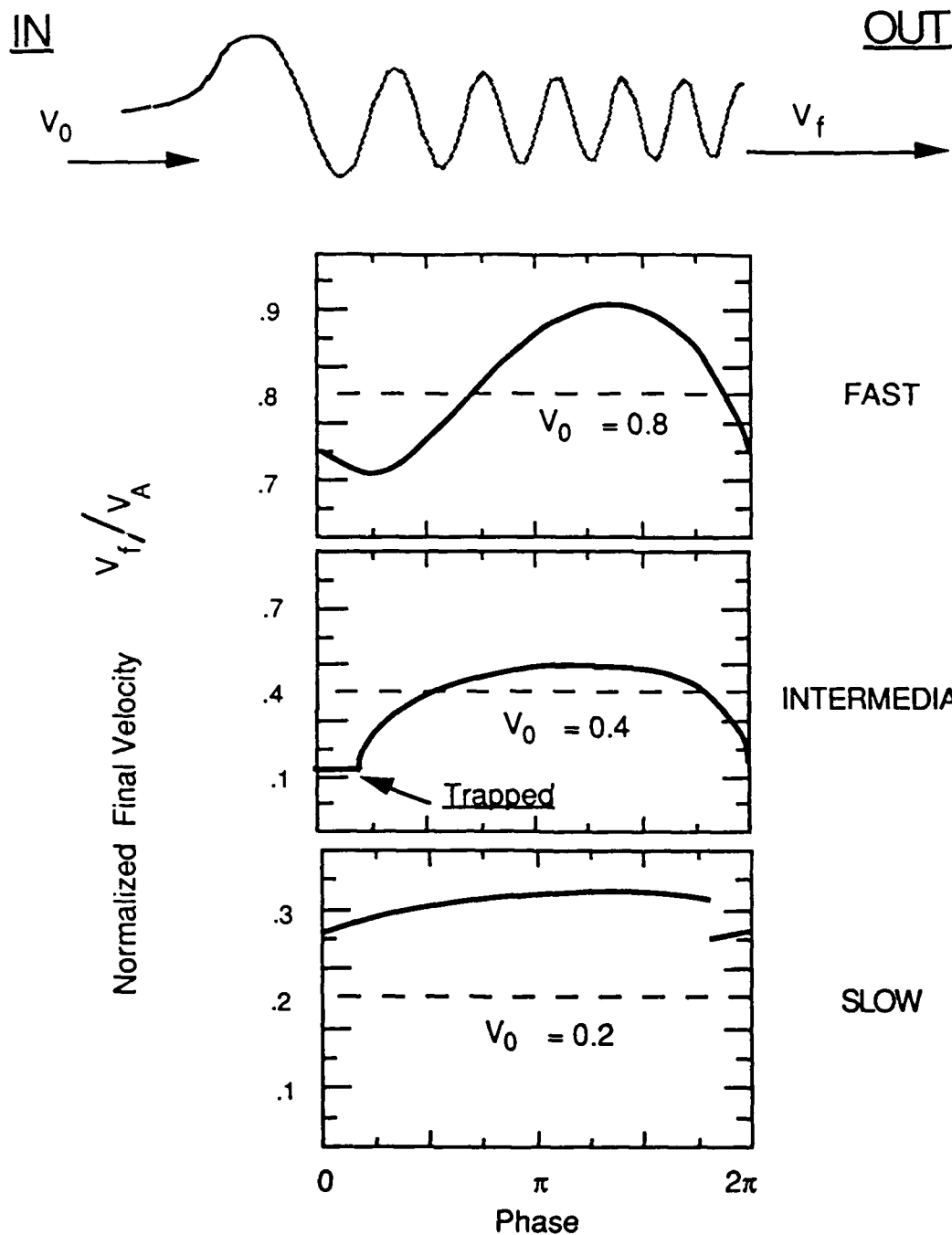
Figure 12. The behavior of the velocity change as a function of initial velocity and initial wave phase depends strongly upon the initial velocity of the particle.

few particles that can be trapped, however, exhibit deceleration as they adiabatically follow the decreasing wave phase velocity.

Eventually, at some value of z, the adiabatic invariant associated with the oscillatory trapped motion[18] is violated and the particle escapes. Perhaps the most interesting and important category of interaction is experienced by the slow particles. Every one of these particles is found to be accelerated, independently of the initial wave phase. Clearly, energizing the entire population of slow particles should cause catastrophic damping of the wave.

The dependence of the asymptotic velocity v_f on the wave phase of a particle injected on the overdense side of plasma resonance with velocity v_0 is shown in Fig. 12. The top panel corresponds to fast particles ($v_0 = 0.8 \ v_A$) and exhibits a nearly sinusoidal behavior, characteristic of diffusive behavior (i.e., some phases result in energy gain and others energy reduction). The middle panel shows the behavior of intermediate velocity ($v_0 = 0.4 \ v_A$) particles. The constant step on the left side corresponds to the trapped particles that have been decelerated by the wave. The bottom panel shows clearly that slow particles ($v_0 = 0.2 \ v_A$)
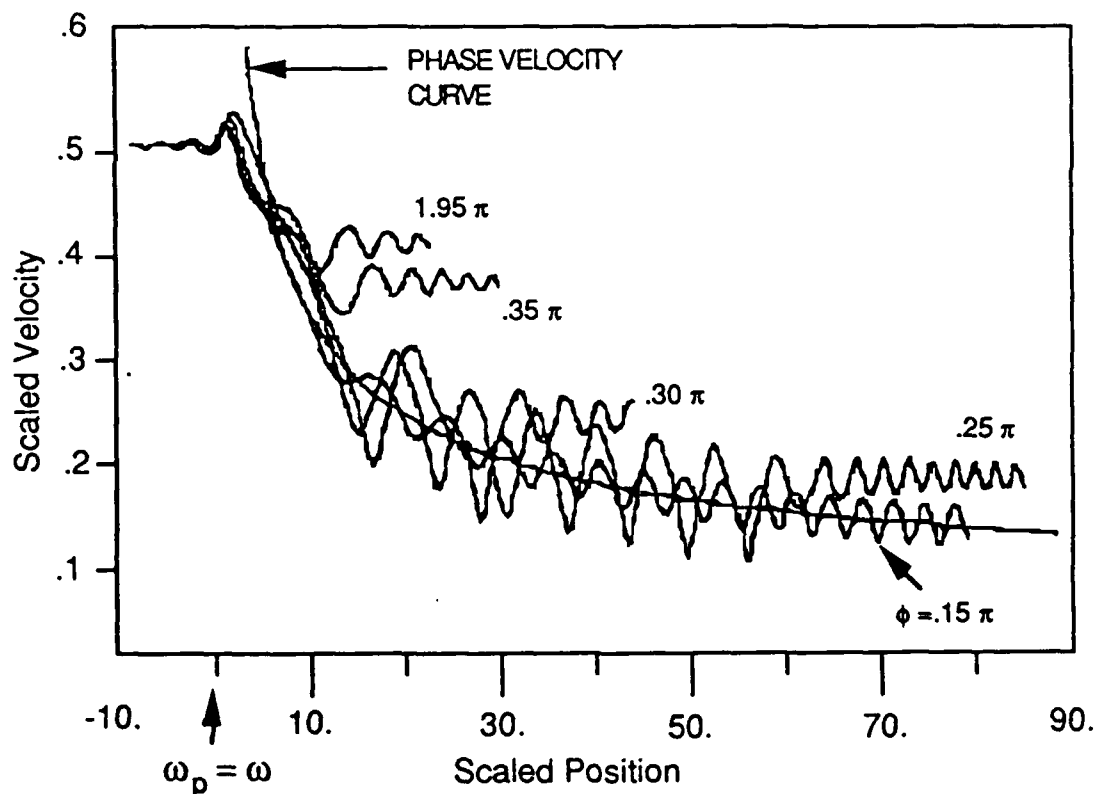

Figure 13. The trapping of particles by the resonant field is only temporary and occurs only over a narrow range of intitial phases.

experience a velocity increase for all wave phases.

The transient nature of the trapping process is exhibited in Fig. 13 which shows the phase trajectories of particles with initial velocity $0.5v_A$ for those wave phases which result in entrainment. It is evident that a small phase change results in significantly different detrapping positions.

The physical process responsible for the phase-independent acceleration of slow particles is illustrated in Fig. 14. Essentially, if the particle has the wrong phase to experience acceleration when first encountering the wave it is slowed down at a rate
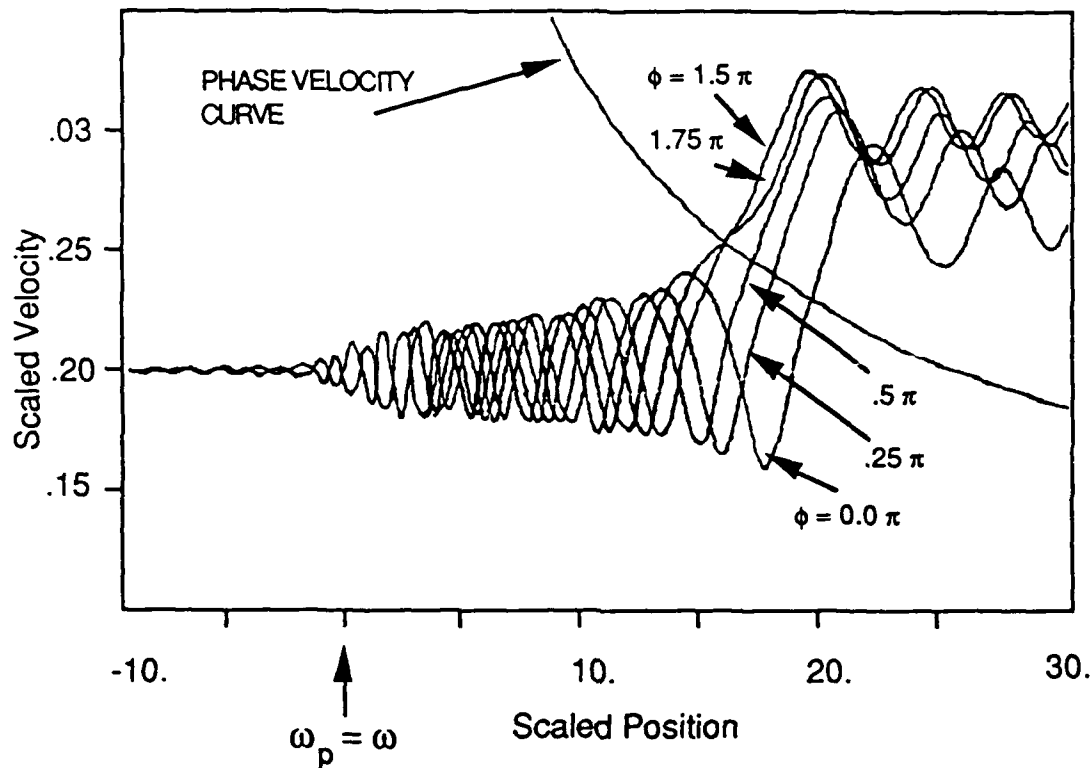
Figure 14. All slow particles are accelerated independently of the initial wave phase.

faster than the decrease in wave phase velocity, and thus immediately re-encounters the wave with a phase that results in acceleration. Once acceleration occurs, the particle does not come into resonance with the wave again because the wave phase velocity continues to decrease with position.

REFERENCES

1. R. C. Davidson, "Methods in Nonlinear Plasma Theory", W. A. Benjamin, Inc. (1974).
2. "Reviews of Plasma Physics", M. A. Leontovich, Ed., Vol. 7 Consultants Bureau (1979).
3. "Handbook of Plasma Physics", M. N. Rosenbluth and R. Z. Sagdeev, Eds., Vol. 2, North Holland Publishing Co. (1983).
4. R. P. Drake, Phys. Fluids B, $\underline{2}$, 225 (1990).
5. A. Simon and R. W. Short, Phys. Fluids B, $\underline{2}$, 227 (1990).
6. R. L. Showen and D. M. Kim, J. Geophys. Res., $\underline{83}$, 623 (1978).
7. P. Stubbe, H. Kopka, H. Lauche, M. T. Rietveld, A. Brekke, O. Holt, T. B. Jones, T. Robinson, A. Hedberg, B. Thide, M. Crochet and H. J. Lotz, J. Atmos. Terr. Phys., $\underline{44}$, 1025 (1982).
8. B. Thide, H. Derblom, A. Hedberg, H. Kopka and P. Stubbe, Radio Science, $\underline{18}$, 851 (1983).
9. A. D. Johnstone and J. D. Winningham, J. Geophys Res, $\underline{87}$, 2321 (1982).
10. D. E. Hinkel-Lipsker, B. D. Fried and G. J. Morales., Phys. Rev. Lett., $\underline{62}$, 2680 (1989).
11. J. E. Maggs and G. J. Morales, J. Plasma Phys., $\underline{41}$, 301 (1989).
12. A. Y. Wong, G. J. Morales, D. E. Eggleston, J. Santoru and R. Behnke, Phys. Rev. Lett., $\underline{47}$, 1340 (1981).
13. G. J. Morales, M. M. Shoucri and J. E. Maggs, Phys. Fluids, $\underline{31}$, 1471 (1988).
14. M. M. Shoucri, G. J. Morales and J. E. Maggs, J. Geophys. Res., $\underline{92}$, 246 (19870.
15. G. J. Morales and J. E. Maggs, Phys. Fluids, $\underline{31}$, 3807 (1988).
16. M. N. Rosenbluth and C. S. Liu, Phys. Rev. Lett., $\underline{29}$, 701 (1972).
17. J. E. Maggs and G. J. Morales, UCLA PPG-Report 1283, Feb. (1990).
18. G. Laval and R. Pellat, J. Geophys. Res., $\underline{73}$, 3255 (1968).

PPG-1280   "Unconventional FEL's," John M. Dawson, presented at SPIE OS/LASE '90 meeting, January 1990.

PPG-1281   "Auroral Kilometric Radiation: An Example of Relativistic Wave-Particle Interaction in Geoplasma, " P. L. Pritchett, to be published in Phys. of Space Plasmas (1989), SPI Conference Proceedings and Reprint Series, #9, January, 1990.

PPG-1282   "Localized Density Clumps and Potentials Generated in a Magnetized Non-Neutral Plasma," G. Rosenthal and A.Y. Wong, sub. to PRL, February 1990.

PPG-1283   "Nonlinear Dynamics of Electrons Accelerated by Resonant Fields in Nonuniform Plasmas," J.E. Maggs and G.J. Morales, February 1990.

PPG-1284   "Observation of Induced Currents from Electrodynamic Tethers in a Laboratory Plasma," J.M. Urrutia and R. Stenzel, sub. to GRL, February 1990.

PPG-1285   "Ionospheric Modification--An Outdoor Laboratory for Plasma and Atmospheric Science," A.Y. Wong and R.G. Brandt, sub. to Radio Science, February 1990.

PPG-1286   "Three-Dimensional Gyrokinetic Particle Simulation of Low-Frequency Drift Instabilities", R.D. Sydora, invited paper presented at Thirty-First APS meeting, February, 1990.

PPG-1287   "Report on High Power Density Fusion Systems by Magnetic Fusion Advisory Committee Panel and Capital X", R. Conn, May 1985.

PPG-1288   "On the Amplification Mechanism of the Ion-Channel Laser," K.R. Chen, T. Katsouleas, and J.M. Dawson, sub. to IEEE Trans. Plasma Sci., February 1990.

PPG-1289   "Pressure-Driven Sound Turbulence in a High Beta Plasma," R. Stenzel, sub. to Phys. Rev. Lett., March 1990.

PPG-1290   "Burn Threshold for Fusion Plasmas with Helium Accumulation," R.J. Taylor, B.D. Fried, and G.J. Morales, sub. to Comments on Plasma Physics and Controlled Fusion, March 1990.

PPG-1291   "Experimental Evidence for Coupling of Plasma Particle and Heat Transport in TEXT", B.L. Brower, S. K Kim, W. Wenzel submitted to Phy. Rev Lett , January 1990.

PPG-1292   "Heating of the Polar Wind Due to Ion Beam Instabilities," M.W. Chen and M. Ashour-Abdalla, sub. to JGR, March 1990.

PPG-1293   "Force Free Electromagnetic Pulses in a Laboratory Plasma," by R. Stenzel and J. M. Urrutia, sub. to Phys. Rev. Letters, March 1990.

PPG-1294   "Scaling Laws of Toroidally Coupled RF Driven Field-Reversed Configurations," A. Kuthi, presented at US/Japan Workshop on Field-Reversed Configurations (November 1989), March 1990.

PPG-1295 "Physics Modeling of Tokamak Transport, A Grand Challenge for Controlled Fusion," J.M. Dawson, R.D. Sydora, and V.K. Decyk, April 1990.

PPG-1296 "Inverse Mode Conversion of Ion Bernstein Waves in Tokamak Plasmas," H. Romero and G.J. Morales, April 1990.

PPG-1297 "Kinetic Nonlinearities in Nonuniform Plasmas," G.J. Morales and J.E. Maggs, Invited Paper at Topical Conference on Research Trends in Nonlinear and Relativistic Effects in Plasmas, La Jolla, CA; Feb. 5-8, 1990; April 1990.

PPG-1300 "Executive Summary of the AIRES-I Reactor Design," R.W. Conn, S. Najamabadi, et al., March 1990.

PPG-1301 "ISIS MFECC Version User Manual", J. J. Su, July, 1989.